

# Ruthenium Olefin Metathesis Catalysts Bearing an *N*-Fluorophenyl-*N*-Mesityl-Substituted Unsymmetrical *N*-Heterocyclic Carbene

Georgios C. Vougioukalakis and Robert H. Grubbs\*

Arnold and Mabel Beckman Laboratory of Chemical Synthesis, Division of Chemistry and Chemical Engineering, California Institute of Technology, Pasadena, California 91125

Received November 17, 2006

**Summary:** Two new ruthenium-based olefin metathesis catalysts, each bearing an unsymmetrical *N*-heterocyclic carbene ligand, have been synthesized and fully characterized. Their catalytic performance has been evaluated in ring-closing metathesis, cross metathesis, and ring-opening metathesis polymerization reactions.

## Introduction

The development of well-defined catalysts with good functional group tolerance has established olefin metathesis as a powerful tool for the formation of carbon–carbon double bonds.<sup>1</sup> In particular, catalysts (PCy<sub>3</sub>)<sub>2</sub>Cl<sub>2</sub>Ru=CHC<sub>6</sub>H<sub>5</sub> (**1**, Figure 1)<sup>2</sup> and (H<sub>2</sub>IMes)(PCy<sub>3</sub>)Cl<sub>2</sub>Ru=CHC<sub>6</sub>H<sub>5</sub> (**2**, Figure 1),<sup>3</sup> along with the phosphine-free second-generation catalyst (H<sub>2</sub>IMes)Cl<sub>2</sub>Ru=CH(*o*-iPrO–Ph) (**3**, Figure 1),<sup>4</sup> have been extensively used in both organic and polymer chemistry due to their high reactivity with olefinic substrates in the presence of most common functional groups. Moreover, numerous other ruthenium-based complexes that can mediate ring-closing metathesis (RCM), cross metathesis (CM), and ring-opening metathesis polymerization reactions (ROMP) have been studied to date. Nevertheless, the development of catalysts that can efficiently control *E/Z* selectivity in CM reactions, or afford tetrasubstituted double-bond products in RCM reactions, still represents a major challenge.

The use of unsymmetrically substituted *N*-heterocyclic carbene (NHC) ligands is one of the modifications that have been reported for the NHC-containing ruthenium metathesis initiators.<sup>5–8</sup> The incentive to exploit unsymmetrical NHCs was initially based on the anticipation that the unsymmetrical nature of these ligands might alter the environment of key intermediates in the metathesis pathway, leading to improved *E/Z* selectivity in CM

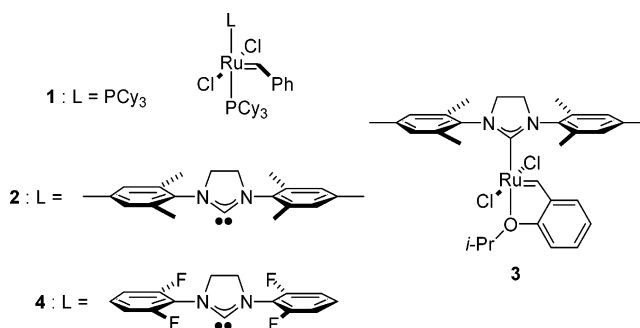


**Figure 1.** Ruthenium-based olefin metathesis catalysts **1–4**.

reactions and diastereoselectivity in RCM reactions.<sup>7</sup> Moreover, although it is not yet absolutely clear to what extent and via which way the electron density that is transferred from the carbenic center of NHCs to the metal affects the catalyst efficiency,<sup>9</sup> the enhanced electron-donating ability of alkyl substituents was anticipated to lead to increased catalyst activity.<sup>6,8</sup> To date, apart from the bidentate asymmetric ligand developed by Hoveyda and co-workers,<sup>10</sup> all reported saturated unsymmetrical NHCs bear one alkyl and one mesityl side group on the two nitrogen atoms of the imidazolium ring.<sup>6–8</sup>

Additionally, a recent report from our group disclosed a significant rate enhancement in the catalytic performance of ruthenium catalyst **4** (Figure 1) bearing *o*-fluorinated aryl groups on the NHC ligand, possibly due to a fluorine–ruthenium interaction.<sup>11</sup> This uncommon interaction, observed in the solid-state structure of **4**, prompted us to develop unsymmetrical catalysts **5** and **6** (Figure 2), bearing the 1-(2,6-difluorophenyl)-3-(mesityl)-4,5-dihydroimidazolin-2-ylidene ligand. We antici-

\* Corresponding author. E-mail: rhg@caltech.edu.

(1) Grubbs, R. H. *Handbook of Metathesis*; Wiley-VCH: Weinheim, Germany, 2003.

(2) (a) Schwab, P.; France, M. B.; Ziller, J. W.; Grubbs, R. H. *Angew. Chem., Int. Ed. Engl.* **1995**, *34*, 2039–2041. (b) Schwab, P.; Grubbs, R. H.; Ziller, J. W. *J. Am. Chem. Soc.* **1996**, *118*, 100–110.

(3) Scholl, M.; Ding, S.; Lee, C. W.; Grubbs, R. H. *Org. Lett.* **1999**, *1*, 953–956.

(4) (a) Kingsbury, J. S.; Harrity, J. P. A.; Bonitatebus, P. J., Jr.; Hoveyda, A. H. *J. Am. Chem. Soc.* **1999**, *121*, 791–799. (b) Garber, S. B.; Kingsbury, J. S.; Gray, B. L.; Hoveyda, A. H. *J. Am. Chem. Soc.* **2000**, *122*, 8168–8179.

(5) Fürstner, A.; Ackermann, L.; Gabor, B.; Goddard, R.; Lehmann, C. W.; Mynott, R.; Stelzer, F.; Thiel, O. R. *Chem.–Eur. J.* **2001**, *7*, 3236–3253.

(6) Dinger, M. B.; Nieczypor, P.; Mol, J. C. *Organometallics* **2003**, *22*, 5291–5296.

(7) Vehlou, K.; Maechling, S.; Blechert, S. *Organometallics* **2006**, *25*, 25–28.

(8) Ledoux, N.; Allaert, B.; Pattyn, S.; Mierde, H. V.; Vercaemst, C.; Verpoort, F. *Chem.–Eur. J.* **2006**, *12*, 4654–4661.

(9) The catalytic activity of ruthenium-based metathesis catalysts has been shown to depend on the electronic properties of *p*-substituents on the phenyl ring of NHCs. This transfer of electronic information into the ruthenium center was proposed to occur through space: (a) Süßner, M.; Plenio, H. *Chem. Commun.* **2005**, 5417–5419. It has been also found that, in a series of Ni(CO)<sub>3</sub>(NHC) complexes, alkyl-substituted NHCs are only slightly more electron donating than aryl-substituted ones and that saturated NHCs are somewhat less electron donating than their unsaturated analogues: (b) Dorta, R.; Stevens, E. D.; Scott, N. M.; Costabile, C.; Cavallo, L.; Hoff, C. D.; Nolan, S. P. *J. Am. Chem. Soc.* **2005**, *127*, 2485–2495. For another classification of the relative  $\sigma$ -donor/ $\pi$ -acceptor properties of a series of NHC ligands see: (c) Herrmann, W. A.; Schütz, J.; Frey, G. D.; Herdtweck, E. *Organometallics* **2006**, *25*, 2437–2448.

(10) (a) Van Veldhuizen, J. J.; Garber, S. B.; Kingsbury, J. S.; Hoveyda, A. H. *J. Am. Chem. Soc.* **2002**, *124*, 4954–4955. (b) Van Veldhuizen, J. J.; Gillingham, D. G.; Garber, S. B.; Kataoka, O.; Hoveyda, A. H. *J. Am. Chem. Soc.* **2003**, *125*, 12502–12508. (c) Gillingham, D. G.; Kataoka, O.; Garber, S. B.; Hoveyda, A. H. *J. Am. Chem. Soc.* **2004**, *126*, 12288–12290. (d) Van Veldhuizen, J. J.; Campbell, J. E.; Giudici, R. E.; Hoveyda, A. H. *J. Am. Chem. Soc.* **2005**, *127*, 6877–6882.

(11) Ritter, T.; Day, M. W.; Grubbs, R. H. *J. Am. Chem. Soc.* **2006**, *128*, 11768–11769.

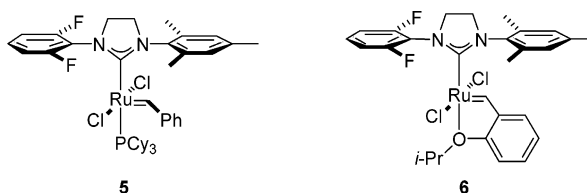
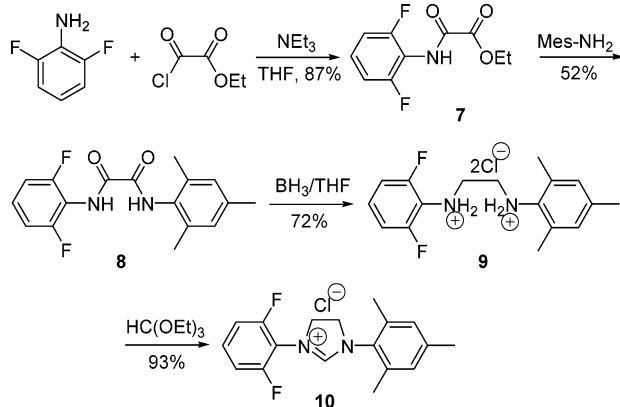


**Figure 2.** New, ruthenium-based metathesis catalysts **5** and **6** bearing an unsymmetrical NHC ligand.

**Scheme 1. Synthesis of the Unsymmetrical 4,5-Dihydroimidazolium Chloride Carbene Precursor 10**



pated not only that replacing a 2,6-difluorophenyl group, in complex **4**, with a mesityl group would lead to a more stable catalyst,<sup>12</sup> maintaining the high activity of the tetrafluorinated complex, but also that the unsymmetrical nature of the NHC, together with a possible fluorine–ruthenium interaction,<sup>13</sup> would have a positive impact on its stereoselectivity in olefin metathesis reactions.

As illustrated in Scheme 1, the synthesis of 1-(2,6-difluorophenyl)-3-(mesityl)-4,5-dihydroimidazolium chloride was straightforward, following a modification of a previously reported synthetic pathway.<sup>14</sup> Reaction of commercially available 2,6-difluoroaniline with ethylchlorooxalacetate affords the oxalamic acid ethyl ester **7**, which, upon condensation with mesitylaniline, gives the corresponding oxalamide **8**. Reduction of **8** with  $\text{BH}_3\cdot\text{THF}$  complex furnishes dihydrochloride salt **9**, which cyclizes upon treatment with triethyl orthoformate to imidazolium chloride **10**. Complex **5** was isolated in 83% yield by generation of the free carbene from **10**, *in situ* with KHMDS, and reaction with ruthenium source **1** in benzene. Treatment of **5** with *o*-isopropoxy- $\beta$ -methylstyrene afforded the phosphine-free analogue **6** in 74% yield after crystallization. Complexes **5** and **6** are both air stable in the solid state and can be purified by silica gel chromatography.

Compounds **5** and **6** were completely characterized by NMR and HRMS, as well as single-crystal X-ray analysis (Figures 3 and 4). In solution, the NHC of complex **6** rotates fast around the Ru–C<sub>NHC</sub> bond on the NMR time scale (only one benzylidene peak is observed) even at  $-70\text{ }^\circ\text{C}$ . On the other hand, complex **5**, in solution, is a mixture of two conformational

(12) The phosphine-containing tetrafluorinated catalyst is less stable than the  $\text{H}_2\text{IMes}$  parent complex **2**. For a recent decomposition study in ruthenium-catalyzed olefin metathesis reactions see: Hong, S. H.; Day, M. W.; Grubbs, R. H. *J. Am. Chem. Soc.* **2004**, *126*, 7414–7415.

(13) (a) Perera, S. D.; Shaw, B. L. *Inorg. Chim. Acta* **1995**, *228*, 127–131. For related review articles see: (b) Kiplinger, J. L.; Richmond, T. G.; Osterberg, C. E. *Chem. Rev.* **1994**, *94*, 373–431. (c) Kulawiec, R. J.; Crabtree, R. H. *Coord. Chem. Rev.* **1990**, *99*, 89–115.

(14) Waltman, A. W.; Grubbs, R. H. *Organometallics* **2004**, *23*, 3105–3107.

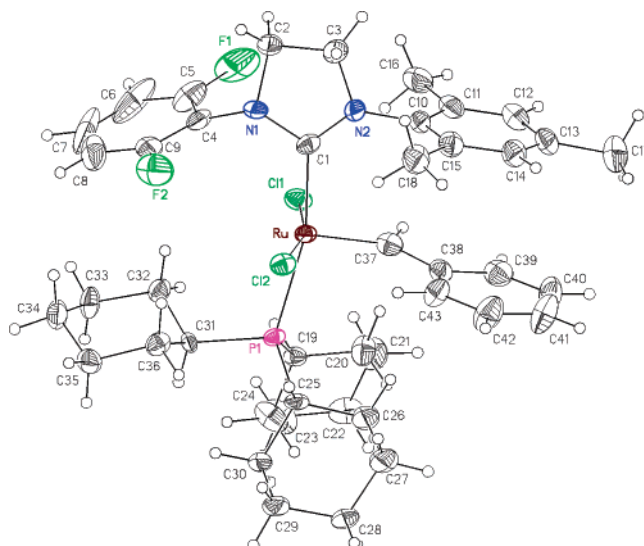


**Figure 3.** X-ray structure of **5** with 50% probability ellipsoids.

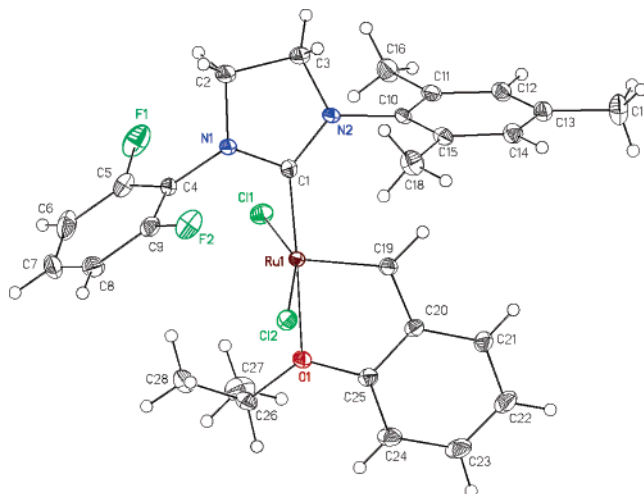


**Figure 4.** X-ray structure of **6** with 50% probability ellipsoids.

isomers (22/82 ratio at room temperature, *vide infra*) as a result of the NHC ligand rotation. In the  $^1\text{H}$  NMR spectrum the benzylidene protons resonate at  $\delta$  19.42 (s, minor rotamer) and 19.14 ppm (s, major rotamer), whereas  $^{31}\text{P}$  NMR shows one singlet resonance for each of the isomers at  $\delta$  31.54 (minor rotamer) and 27.54 ppm (major rotamer). From the temperature dependence of the equilibrium constant (van't Hoff plot) we calculated the energy difference for the two rotamers of **5**.<sup>15</sup> The major rotamer was found to be  $4.4 \pm 0.1$  and  $4.7 \pm 0.3$   $\text{kJ}\cdot\text{mol}^{-1}$  lower in energy than the minor species, in  $\text{CD}_2\text{Cl}_2$  and toluene- $d_8$ , respectively (SI). Thus far, it has been impossible to obtain any diagnostic information regarding the orientation of the NHC in the two rotational isomers from NOE experiments in solution. However, comparison of the  $^1\text{H}$  NMR chemical shifts in the two rotamers of **5** with the diagnostic chemical shifts for the methine-H of the benzylidene, the *m*-H, and the *o*- and *p*- $\text{CH}_3$  groups of the mesityl ring in complex **2**,<sup>16</sup> suggests that the major rotational isomer contains a mesityl ring located above the benzylidene group. We also acquired a low-temperature  $^1\text{H}$  NMR spectrum ( $-70\text{ }^\circ\text{C}$ ,  $\text{CD}_2\text{Cl}_2$ ) of the single crystals studied by X-ray crystallography, containing only

(15) Dwyer, C. L.; Kirk, M. M.; Meyer, W. H.; van Rensburg, W. J.; Forman, G. S. *Organometallics* **2006**, *25*, 3806–3812.

(16) Sanford, M. S. Ph.D. Thesis, California Institute of Technology, Pasadena, 2001.

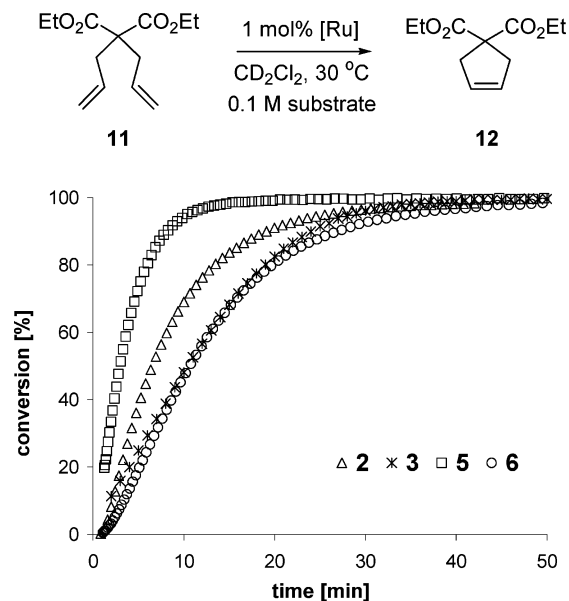


Figure 5. RCM of diene **11** to disubstituted cycloalkene **12**.

the rotamer presented in Figure 3. This spectrum showed a 5/95 ratio for the two benzyldiene protons, as compared to the room-temperature ratio of 22/82, providing additional evidence for the assignment described above. The energy difference between the two rotational isomers may arise from the more efficient slipped  $\pi$ - $\pi$  stacking interaction of the benzyldiene moiety with the *N*-mesityl than with the *N*-(2,6-difluorophenyl) group.<sup>17</sup>

Activation parameters for the NHC rotation in **5** were estimated by using <sup>1</sup>H NMR spectroscopy, following the broadening and coalescence of the methine protons of the benzyldiene group, and by using the Eyring plot of the corresponding rates of interconversion, obtained by line shape simulations. The free energy of activation for the interconversion of the two rotational isomers, estimated at 25 °C, is  $\Delta G^{\ddagger 298} = 17.9 \pm 0.1 \text{ kcal}\cdot\text{mol}^{-1}$  [ $\Delta H^{\ddagger} = 19.6 \pm 0.7 \text{ kcal}\cdot\text{mol}^{-1}$  and  $\Delta S^{\ddagger} = 6 \pm 2 \text{ cal}\cdot\text{mol}^{-1}\cdot\text{K}^{-1}$ ], almost 4 kcal·mol<sup>-1</sup> lower than the corresponding barrier to rotation in complex **2** [ $\Delta G^{\ddagger 298} = 21.8 \pm 0.3 \text{ kcal}\cdot\text{mol}^{-1}$ ].<sup>16</sup> These results show that fluorine substituents, instead of slowing down the NHC rotation by a potential F-association, induce a speed increment most likely due to their decreased steric bulk.

With complexes **5** and **6** in hand, we studied their catalytic activity in the RCM reactions of diethyl diallyl malonate (**11**, Figure 5), diethylallylmethyl malonate (**13**, Figure 6), and diethyl dimethyl malonate, according to literature procedures.<sup>18</sup> The plots of cycloalkene **12** concentration versus time for the RCM of **11** by catalysts **2**, **3**, **5**, and **6**, in Figure 5, reveal that complex **5** effects the cyclization of **11** with an increased reaction rate compared to catalysts **2**, **3**, and **6**. Furthermore, catalysts **3** and **6** are almost indistinguishable in their catalytic activity toward **11**, catalyzing the reaction at a slower rate than both **2** and **5**. The rate enhancement in the RCM of **11**, by the phosphine-containing unsymmetrical catalyst **5**, may be due to

(17) Review articles on  $\pi$ - $\pi$  stacking interactions: (a) Williams, J. H. *Acc. Chem. Res.* **1993**, *26*, 593–598. (b) Janiak, C. J. *Chem. Soc., Dalton Trans.* **2000**, 3885–3896. For a more recent example of intramolecular  $\pi$ - $\pi$  stacking interactions see: (c) Mandal, D.; Gupta, B. D. *Organometallics* **2006**, *25*, 3305–3307. (d) Mandal, D.; Gupta, B. D. *Organometallics* **2007**, *26*, 658–670.

(18) All reactions were performed at least in duplicate to confirm reproducibility. For experimental procedures see: Ritter, T.; Hejl, A.; Wenzel, A. G.; Funk, T. W.; Grubbs, R. H. *Organometallics* **2006**, *25*, 5740–5745.

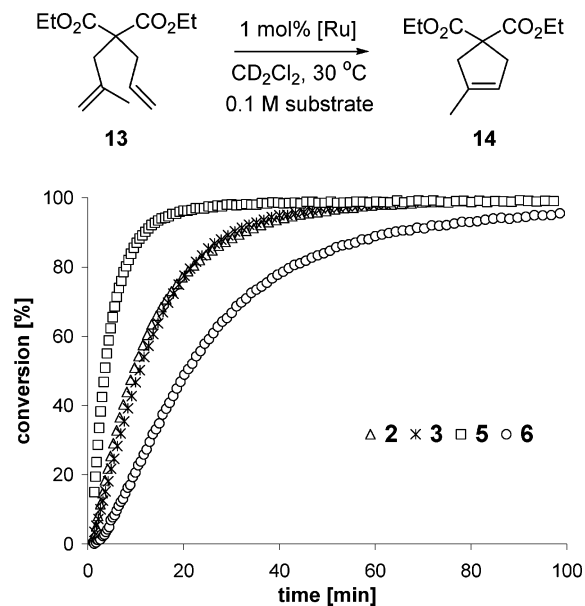


Figure 6. RCM of diene **13** to trisubstituted cycloalkene **14**.

a fluorine–ruthenium interaction.<sup>11</sup> Gratifyingly, one of the primary objectives that guided us in this research, namely, to synthesize a more stable catalyst than **4**, was also accomplished. Thus, the RCM reaction of **11** follows pseudo-first-order reaction kinetics, as illustrated by the linear logarithmic plot of diene concentration versus time. In contrast, catalyst **4** shows a curvature in the corresponding logarithmic plot indicating a decreasing activity during the course of the reaction.

As depicted in Figure 6, regarding the more challenging RCM of substrate **13**, catalyst **5** once more surpasses catalysts **2**, **3**, and **6**. In the RCM formation of this more demanding trisubstituted double bond though, catalyst **6** is significantly less efficient even than the second-generation complexes **2** and **3**. This is most likely due to its longer induction period, i.e., slower catalyst initiation, as illustrated in the shape of the curve for the progression of the RCM formation of **14**.

RCM of diethyl dimethyl malonate, affording a cyclic olefin with a tetrasubstituted double bond, is an even more challenging model reaction, again due to the increased steric bulk of the substrate, requiring high catalyst loadings and elevated reaction temperatures. Catalyst **5** is the most efficient in the present study, affording 30% of the ring-closed product after 4 days at 30 °C. Complexes **2**, **3**, and **6** catalyze the same reaction in 17, 6, and 9% yields, respectively.

Subsequent initiation studies, utilizing the reaction between **5** and butyl vinyl ether, revealed an approximately 4-fold increase in the initiation rate of catalyst **5** relative to **2** (SI). This reaction is rapid, quantitative, and irreversible, affording the corresponding Fischer carbene. Moreover, it generally proceeds with clean kinetics and can be easily analyzed by <sup>1</sup>H NMR spectroscopy.<sup>19</sup> The reaction constant,  $k_{\text{obs}} = (1.7 \pm 0.1) \times 10^{-3} \text{ s}^{-1}$  [catalyst **2**:  $k_{\text{obs}} = (4.6 \pm 0.4) \times 10^{-4} \text{ s}^{-1}$ ], was found to be independent of olefin concentration relative to [Ru] over an olefin concentration range of 0.15 to 1.35 M. This implies that saturation conditions are achieved even at relatively low concentrations of olefinic substrate and, therefore, suggests rate-determining phosphine dissociation. The large and positive values for  $\Delta H^{\ddagger}$  [(27 ± 2) kcal·mol<sup>-1</sup>] and  $\Delta S^{\ddagger}$  [(19 ± 9) cal·mol<sup>-1</sup>·K<sup>-1</sup>], obtained from the temperature dependence of

(19) (a) Sanford, M. S.; Ulman, M.; Grubbs, R. H. *J. Am. Chem. Soc.* **2001**, *123*, 749–750. (b) Sanford, M. S.; Love, J. A.; Grubbs, R. H. *J. Am. Chem. Soc.* **2001**, *123*, 6543–6554.

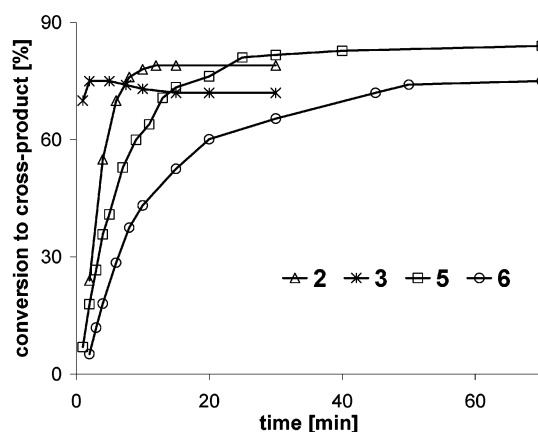
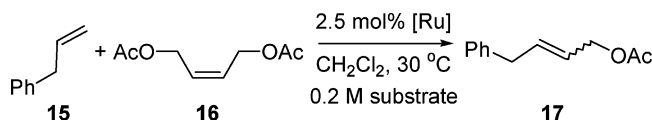


**Figure 7.** Monitoring CM of allyl benzene with *cis*-1,4-diacetoxy-2-butene.

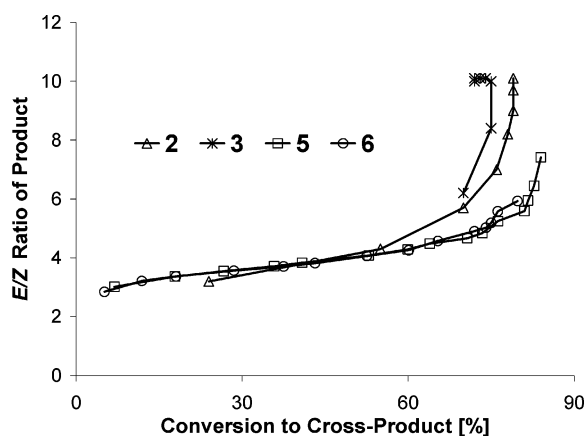


**Figure 8.** *E/Z* ratio of cross-product **17** vs conversion to cross-product **17**.

$k_{\text{obs}}$  at 0.15 M butyl vinyl ether concentration, are also indicative of a dissociative mechanism. The calculated free energy of activation of **5** [ $\Delta G^{\ddagger 298} = 21.78 \pm 0.08 \text{ kcal}\cdot\text{mol}^{-1}$ ] is approximately halfway between that of **2** ( $\Delta G^{\ddagger 298} = 23.0 \text{ kcal}\cdot\text{mol}^{-1}$ )<sup>19</sup> and the  $C_{2v}$  symmetrical tetrafluorinated analogue **4** ( $\Delta G^{\ddagger 298} = 20.4 \text{ kcal}\cdot\text{mol}^{-1}$ ).<sup>11</sup> As expected, the two rotational isomers of **5** decay with the same rate constant, due to the lower barrier to NHC rotation than that to phosphine dissociation.

We also investigated the activity of **5** and **6** in the CM of allyl benzene (**15**) with *cis*-1,4-diacetoxy-2-butene (**16**).<sup>18,20</sup> Catalyst **5** demonstrates activity comparable to that of **2** and **3**, whereas **6** is less efficient due to slow initiation (Figure 7). Interestingly, however, both **5** and **6** give improved *E/Z* ratios of **17** compared to **2** and **3**, at conversions above 60%, as illustrated in the plots of the *E/Z* ratio of cross-product versus conversion to cross-product (Figure 8).

(20) Chatterjee, A. K.; Choi, T. L.; Sanders, D. P.; Grubbs, R. H. *J. Am. Chem. Soc.* **2003**, *125*, 11360–11370.

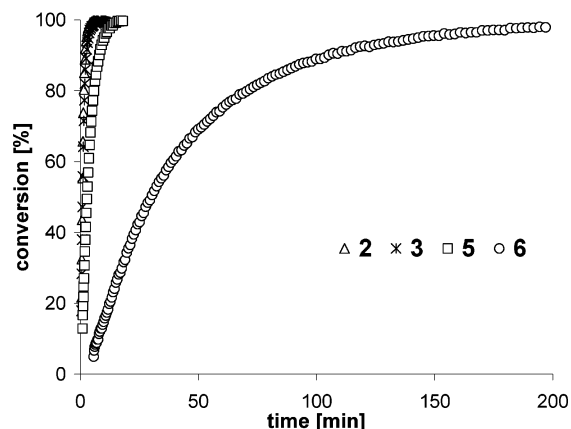
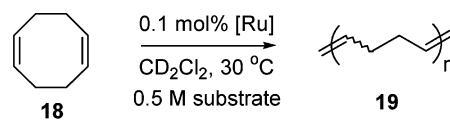


**Figure 9.** Monitoring ROMP of COD.

Last, the catalytic performance of **5** and **6** in the ROMP of 1,5-cyclooctadiene (**18**) was compared with the reactivity of **2** and **3** under similar polymerization conditions (Figure 9).<sup>18</sup> Catalyst **5** shows a slightly lower ROMP activity than **2** and **3**, while **6** is a much less efficient polymerization catalyst due to its prolonged induction period.

In conclusion, ruthenium-based metathesis catalysts **5** and **6** have been synthesized and fully characterized. Their catalytic performance in RCM, CM, and ROMP reactions has been evaluated. The activity of **5** in RCM reactions surpasses that of the commercially available catalysts **2** and **3**. In the same model RCM reactions, the phosphine-free complex **6** demonstrates similar or lower activity than complexes **2** and **3** due to slow initiation. In CM and ROMP model reactions both new catalysts show similar or lower reactivity than **2** and **3**. Interestingly, however, in the CM reaction of allyl benzene with *cis*-1,4-diacetoxy-2-butene, both **5** and **6** give improved *E/Z* selectivity at conversions above 60%. The synthesis of ruthenium-based metathesis catalysts bearing other unsymmetrical NHCs, designed to correlate the observations outlined here, is currently under way.

**Acknowledgment.** The authors would like to thank Larry M. Henling and Dr. Michael W. Day for X-ray crystallographic analysis. Smaranda Marinescu and Prof. John E. Bercaw are acknowledged for assistance with line shape analysis. This research was supported in part by a Marie Curie International Fellowship to G.C.V. within the 6th European Community Framework Programme.

**Supporting Information Available:** Experimental procedures for the synthesis and spectroscopic characterization of all new compounds. Text, tables, figures, and CIF files giving details of the X-ray analysis of catalysts **5** and **6**. Line shape and Eyring analysis for the NHC rotation in catalyst **5**. Initiation kinetics experiments for catalyst **5**. This material is available free of charge via the Internet at <http://pubs.acs.org>.

OM0610593